Metal Phthalocyanines as Catalyst Precursors of Metallated Carbon Nanotubes

Article *in* Recent Patents on Nanotechnology · July 2019

DOI: 10.2174/1872210513666190703120844

3 authors, including:

Oxana V. Kharissova
Autonomous University of Nuevo León
228 PUBLICATIONS **4,558** CITATIONS
SEE PROFILE

Boris I Kharisov
Autonomous University of Nuevo León
297 PUBLICATIONS **6,142** CITATIONS
SEE PROFILE

Send Orders for Reprints to reprints@benthamscience.net

Recent Patents on Nanotechnology, **2019**, *13,* **000-000**

RESEARCH ARTICLE

Metal Phthalocyanines as Catalyst Precursors of Metallated Carbon Nanotubes

Antonio Alanis, Oxana V. Kharissova and Boris I. Kharisov*

Universidad Autónoma de Nuevo León, Ave. Universidad s/n, Ciudad Universitaria, San Nicolás de los Garza, Nuevo León, C.P. 66455, México

ARTICLE HISTORY

Received: November 05, 2018
Revised: December 05, 2018
Accepted: June 13, 2019

DOI:
10.2174/1872210513666190703120844

Abstract: ***Background*****:** The addition of nanoparticles to cellulose paper can improve its mechanical strength, chemical stability, biocompatibility and hydrophobic properties. Silica nanoparticles are known to be inert, hydrophobic, biocompatible, biodegradable and have a good distribution being deposited on surfaces. The main characteristics of 20 nm SiO_2 nanoparticles are good chemical and thermal stability with a melting point of 1610-1728°C, a boiling point of 2230°C with a purity of 99.5%.

Objective**:** To carry out the hydrophobization of paper based on Kraft cellulose and on cellulose obtained from soybean husk with 20-nm size SiO_2 nanoparticles and to study hydrophobicity, morphology and topography of the prepared composites.

Methods**:** The ground and roasted soybean husk was treated with a NaOH, washed and dried. Hydrophobization of paper was carried in aqueous medium by SiO_2 addition in weight ratios "paper-SiO_2 " of 0.01-0.05 wt.%, stirring, filtration and drying. The obtained cellulose sheet composites were characterized by scanning electron microscopy (SEM), transmisión electron microscopy (TEM), FTIR-spectroscopy, Mullen proofs of hydrophobicity, and contact angle measurements.

Results**:** The mechanical properties of paper nanocomposites (tensile strength and compression) increased considerably by varying the concentrations. The tensile strength increased by 41-46% and the compressive strength increased by 55-56%. The existence of fiber nanofoils, good adhesion of 20-nm SiO_2 nanoparticles to the paper surface, and their homogeneous distribution were observed.

Conclusion**:** Cellulose was successfully obtained from soybean husk, applying the alkaline-based extraction method. A good reinforcement of cellulose fibers is observed due to the outstanding characteristics of the silicon dioxide nanoparticles.

Keywords*:* Spray pyrolysis, carbon nanotubes, phthalocyanines, Raman spectroscopy, TEM, SEM.

1. INTRODUCTION

For the carbon nanotubes (CNTs), since their formal rediscovery in 1991 by *Iijima* [1], a number of device applications, such as field-effect transistors, full-color displays, and molecular computers have been envisioned [2,3]. These applications are highly dependent on the electronic properties of the CNTs, which can be tuned by their diameter, helicity, and presence of defects. In the last 2 decades, novel strategies have been devoted to modify physical properties of the CNTs by surface modification with organic, inorganic, and biological species, leading to carbon nanotubes having a number of unique properties. Most of the tubes are semiconductors, but there are excellent conductors (in particular, better than silver) and even insulators.

Methods for carbon nanotubes synthesis are described and reviewed elsewhere, in particular, in a review [4], and generalized in Fig. (**1**). Among them, we note the high-pressure large-scale CNTs synthesis in a autoclave [5], arc discharge [6], electrospinning [7], electrospray deposition [8], and especially various common types of Chemical Vapor Deposition (CVD) methods, in particular radio-field-induced self-bias hot-filament CVD method [9] and a relative plasma-enhanced CVD [10]. The spray pyrolysis [11, 12], as a branch of the CVD, results slightly magnetic CNTs due to presence of nanoparticles of Fe, Ni and other metals, whose compounds-precursors (for example ferrocene $FeCp_2$ in the spray pyrolysis method of CNTs synthesis at 800°C) are used as catalysts for CNTs growth. This synthesis method can be scaled up and can use carbon-containing industrial wastes, for example, tires [13, 14]. At the same time, a permanent search of other possible catalysts for CNTs formation could lead to their unexpected properties and further applications.

*Address correspondence to this author at the Universidad Autónoma de Nuevo León, Ave. Universidad s/n, Ciudad Universitaria, San Nicolás de los Garza, Nuevo León, C.P. 66455, México; E-mail bkhariss@hotmail.com

1872-2105/19 $58.00+.00

Such possible catalysts could be nitrogen-rich metallated macrocycles, for example, porphyrins and phthalocyanines.

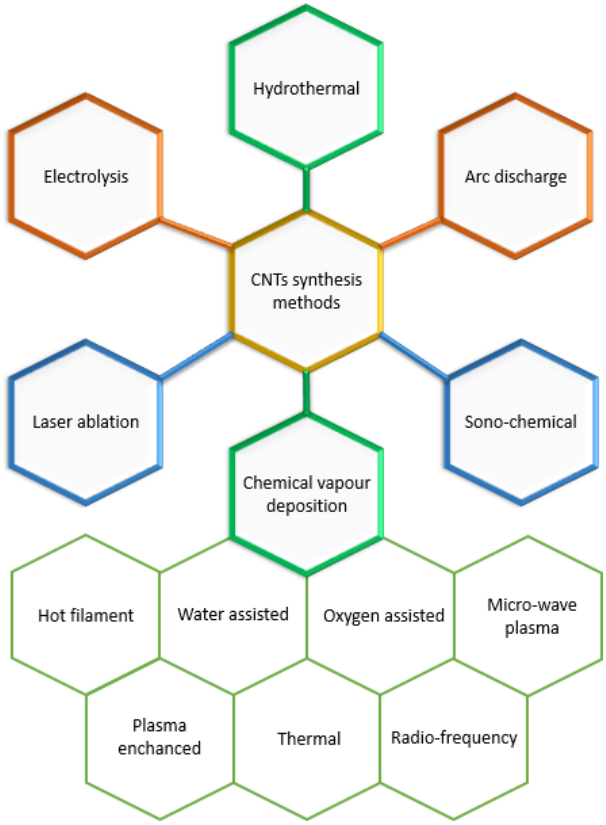

Fig. (1). Currently used methods for CNTs synthesis.

Phthalocyanine-based macrocycle systems (H_2Pc) and their metal complexes (MPc) are promising candidates not only for classic applications, such as, fuel and solar cells, pigments, catalysts, gas sensors, semiconductors, corrosion inhibitors, optical and electronic devices, liquid crystalline materials, but also for nanomaterials design [15, 16]. Their surface chemistry [17] is a relatively young and growing field of research, caused by the versatility of these macromolecules and their metal complexes. MPc are formed with most metallic elements of the *Mendeleev*'s Periodic System and enormous variations in reactivity, electronic and magnetic properties and biological functionality can be found depending on the type of metal center. The phthalocyanine macrocycles are thermally very stable up to 500-800 K, so their thin films can be easily prepared by organic molecular beam epitaxy in a vacuum. These macrocycles possess the conjugated π-extended system and, therefore, share the ability of strong absorption of light in the visible range.

Exploiting the intrinsic optic, electronic, and spintronic properties of novel low-dimensional molecular materials, it is required that the electronic coupling with the supporting substrate is kept as low as possible. In this context, metal-supported ultra-thin insulating films on phthalocyanine basis have attracted great interest as substrates to study the intrinsic properties of organic and inorganic nanostructures. It is also known that several phthalocyanines are capable to form composites with graphene [18] and carbon nanotubes [19], as well as to destroy completely CNTs [20]. Their possible application as metal precursors for CNTs formation could lead to carbon nanotubes containing N-defects on their surface and, as a consequence, other structural and electric properties. However, metal phthalocyanines have not practically been used as catalysts for carbon nanotube formation [21, 22]. In any case, there are no systematic investigations in this field. Metal phthalocyanines have been reported as components for formation of composites [23] with carbon nanotubes to be further used as catalysts [24, 25] and sensors [26]. So, the main goal of this work was the *in situ* study of the formation of thin films from the toluene-phthalocyanine system by spray pyrolysis, characterization of products and search of possible novel applications.

2. EXPERIMENTAL PART

Metal phthalocyanines MPc (M = Cu, Ni, Mg, Zn; 97% purity) were purchased from Sigma-Aldrich Company and used as supplied. Ethanol and toluene were purchased in CTR (Monterrey, Mexico). Electron microscopy images were obtained in SEM and TEM equipment at The University of Texas at Arlington (USA). IR-spectra were measured in ThermoScientific Nicolet equipment. Raman spectra (DXR Raman Microscope ThermoScientific, The University of Texas at Arlington) were collected using an excitation wavelength at 785 nm (1.58 eV).

Using MPc (M = Cu, Ni, Mg, Zn) as metal catalyst precursors, carbon thin films were prepared by a spray pyrolysis technique using the MPc powders, dispersed in **1**) a mixture of toluene and EtOH or, for comparison, **2**) ferrocene solution in a toluene-ethanol mixture. The MPc concentration in each sample was in the range of 0.05 wt.%, 0.5 wt.% and 1 wt.%. Solvent (20 mL, toluene and alcohol, 1:1 vol. mixture) and MPc or solvent (20 mL), ferrocene (0.5 wt.%) and corresponding amounts of MPc were injected to the system at a rate of 1 mL/min in a preheater set to 200°C while nitrogen gas is supplied at a ratio of 1 L/min. After the preheater, the gas passed into a quartz tube, collocated in an oven heated at 760°C. The details of the pyrolysis process are shown in the *Supplementary Material*. This quartz tube contained borosilicate glass substrates, where thin nanofilms were deposited by 20 min (Fig. **2**). Ferrocene in additional experiments was used for comparison with the MPc experiments only. It is known that $FeCp_2$ is a classic catalyst for CNTs formation, meanwhile, MPc could have a double function: it can be a metal catalyst precursor for the formation of CNTs or other carbon nanoparticles and donor of nitrogen for creation of N-defects on CNTs surface.

The samples were characterized by infrared and Raman spectroscopy, scanning electron microscopy (SEM), and transmission electron microscopy (TEM). The electrical measurements were carried out using the technique Kelvin-4 points (4-wires). Special connecting clips (called Kelvin clips) were made to facilitate this kind of connection across a subject resistance (Fig. **3**).

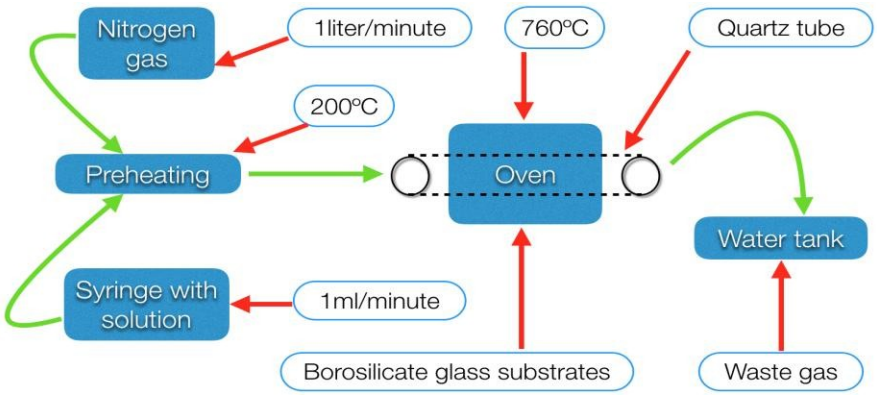

Fig. (2). The spray pyrolysis system.

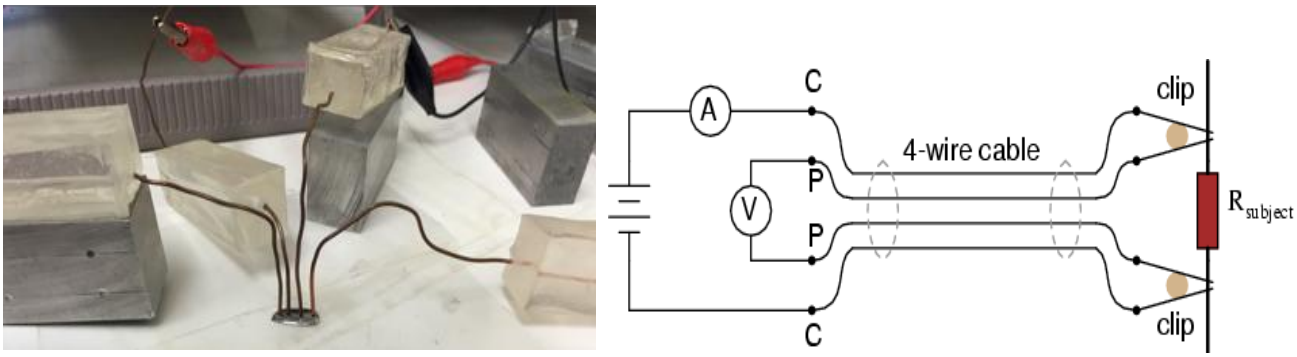

Fig. (3). Kelvin (4 wire sensing) measurements.

Table 1. Deposition parameters and the result of thin film thickness.

Precursor	Concentration (wt.%)	Temperature of Deposition (°C)	Time of Deposition (min)	Thickness (nm)
MgPc	1. 0	760	20	1050
	0.5			481
	0.05			175
NiPc	1.0			3458
	0.5			1037
	0.05			420
CuPc	1.0			439
	0.5			158
	0.05			12
ZnPc	1.0			854
	0.5			857
	0.05			48

3. RESULTS AND DISCUSSION

3.1. Solvent-MPc Mixtures as Precursors

As a result of experiments, the nanometric layers of carbon nanoparticles were deposited on quartz glass due to the catalytic action of the metal nanoparticles, formed from corresponding phthalocyanines by their decomposition. These films were analyzed by scanning and transmission electron microscopy. First, the effect of the mixture of toluene and EtOH with different concentration of dispersed MPc in each sample (0.05 wt.%, 0.5 wt.% and 1 wt.%) was analyzed. As observed in SEM images (Fig. **4**), the morphology and thickness of the thin films vary (Table **1**).

The SEM and TEM data (Fig. 4) show that the MgPc blends allow obtaining the nanoparticles of 5-20 nm sizes (Fig. **4B**) for 0.5 wt.% precursor concentration. The morphology of the deposited particles at concentrations of 0.5 wt. % and 1.0 wt.% is shown in Fig. **4D**. The morphology of the particles of larger sizes (22-37 nm) is present in the samples

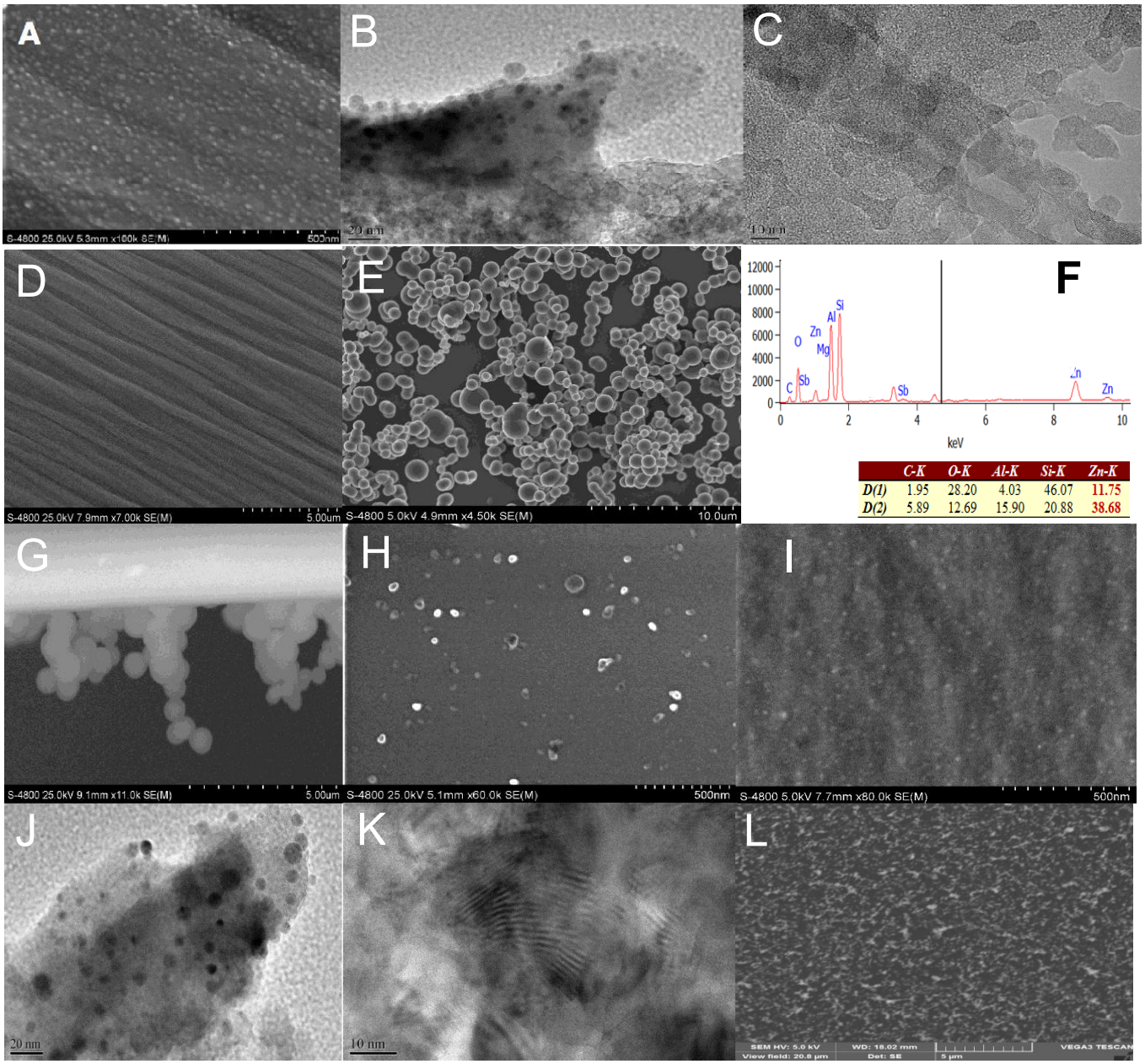

Fig. (4). SEM and TEM images of samples prepared using the following metal phthalocyanine precursors: **A**) SEM (precursor MgPc 0.5 wt.%); **B**) TEM (precursor MgPc 0.5 wt.%); **C**) TEM (precursor MgPc 1.0 wt.%); **D**) SEM (precursor MgPc 1.0 wt.%); **E**) SEM (precursor NiPc 1.0 wt.%); **F**) EDS (precursor ZnPc 1.0 wt.%); **G**) SEM (precursor NiPc 0.5 wt.%); **H**) SEM (precursor NiPc 0.05 wt.%); **I**) SEM (precursor ZnPc 0.05 wt.%); **J**) TEM (precursor ZnPc 0.5 wt.%); **K**) TEM (precursor NiPc 1.0 wt.%); **L**) SEM (precursor ZnPc 1.0 wt.%).

with ZnPc for concentrations 0.05 wt.% (Fig. **4J**) and increases to 285-857 nm for the concentrations of 1.0 wt.% (Fig. **4M**). According to the obtained results, different polymorphic phases of thin carbonaceous films were observed. Structural and morphological changes were found to be dependent on the nature of MPc. SEM data (Fig. **4**) show that MgPc-derived nanoparticles have sizes from 10 to 25 nm (Fig. **4B**) and 20 nm (Fig. **4A**), respectively. In the image profile of the sample of 0.5% NiPc as a precursor (Fig. **4G**), it is shown how the nanoparticles are joined to the surface of the borosilicate glass substrate. They have a size of 10-12 nm of the sample of 0.05% NiPc as a precursor (Fig. **4H**). The diameter of nanoparticles, in case of CuPc used as a precursor, is 15 nm (Fig. **4A**). The thickness of the thin film of the sample was measured to be in the range of 20-1000 nm in case of homogeneous deposition (samples NiPc, CuPc and MgPc); however, in case of the sample Fig. **4E** (ZnPc as a precursor), the deposition was not homogeneous and the thickness varies up to 3400 nm (Table **1**). The TEM data reveals (Fig. **4** y Fig. **5**) that the precursors containing NiPc and CuPc allow obtaining nanoparticles of sizes 5-10 nm (Figs. **5A** and **4H**) for concentrations of 0.05 wt.%, 0.5 wt.% and formation of carbon nanotubes (SWCNTs) with the diameter of 1.25 nm (Fig. **4L** y Fig. **5B**) for concentrations of 1.0 wt.%.

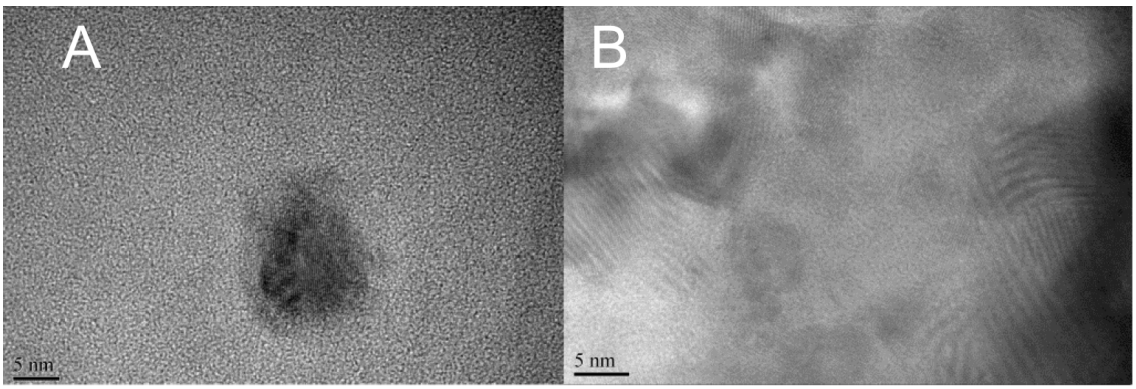

Fig. (5). TEM images of samples prepared using the CuPc precursors: A) TEM (precursor CuPc 0.5 wt.%); B) TEM (precursor CuPc 1.0 wt.%).

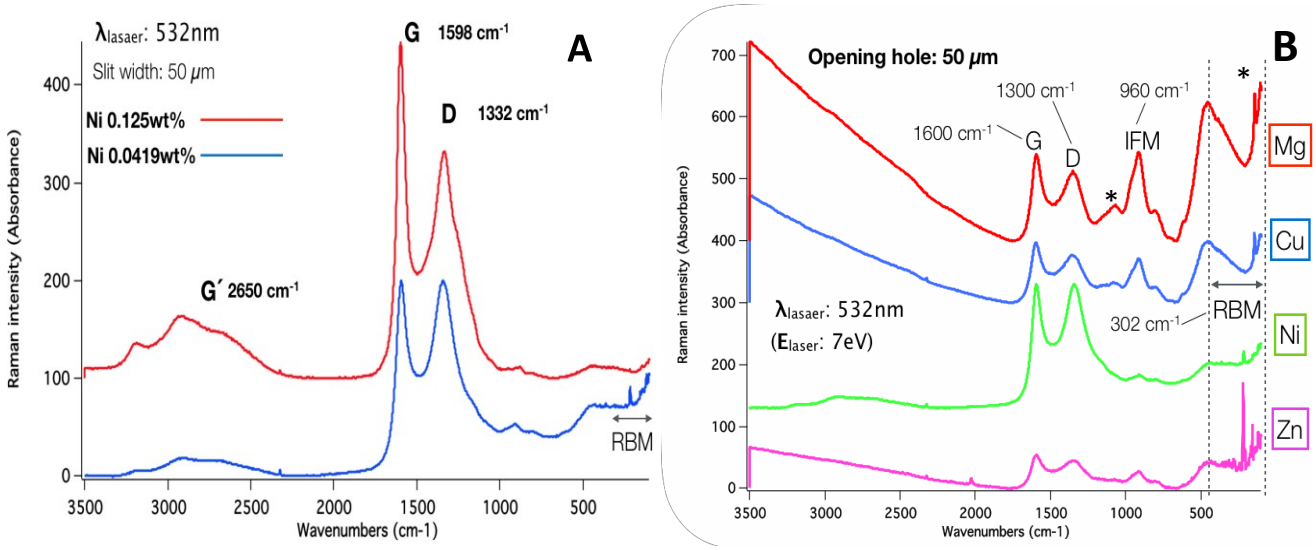

Fig. (6). Raman spectra of thin films: a) comparison of NiPc-derived composites at different concentrations; b) comparison of samples obtained by pyrolysis using different MPc as precursors at 0.5 wt.%. (RBM is Radial Breathing Mode $140 \leq \nu \leq 350$ cm^{-1}) and IFM (intermediate frequency modes IFM^{-} = 750 cm^{-1}, IFM^{+}= 960 cm^{-1}). The features marked with '*' at 248, 521 and 962 cm^{-1} are from the Si/SiO_2 substrate and are used for calibration of the nanotube Raman spectrum [28]).

The Raman spectra of the samples are shown in Fig. (**6**). The radial breathing mode (RBM) at $140 \leq \nu \leq 350$ cm^{-1} are characteristic for SWCNTs; they are clearly present in all samples, together with other carbon nanostructures. The tangential G band at 1600 cm^{-1}, whose profile indicates the metallic or semiconductor character of the CNTs, and the bands D at 1332 cm^{-1} (disorder-induced) and G' at 2650 cm^{-1} (overtone D) are also observed. The band D is indicative of the presence of defects in the walls, so the ratio of intensities of the D and G bands can testify about the number of defects [27]. In the Raman spectrum of samples, in addition to the bands G, D and G', a group of very intense bands centered at 200 cm^{-1} was observed, which are characteristics of SWCNTs ($140 \leq \nu \leq 350$ cm^{-1}) corresponding to the characteristic respiratory mode in radial direction (radial breathing mode RBM) of SWCNTs and inverse linearly depending on the CNT diameter, since the radial breathing mode frequency ν_{RBM} depends linearly on the reciprocal nanotube diameter d_t. They can also correspond to other second-order vibrations as IFM (intermediate frequency modes) at 960 cm^{-1} (weaker bands). The first band D appears at ~1300 cm^{-1}, indicating the disorder of graphite. A strong increase of the band G is seen at 1600 cm^{-1} (vibration mode A1G). In the case of NiPc use (Fig. **6a**), a band at ~2700 cm^{-1} confirms the stacking of graphene layers. The G-band is highly sensitive to strain effects in the sp^2 system and thus can be used to probe modification on the flat surface of graphene.

3.2. Solvent-MPc-ferrocene mixtures as precursors.

The obtained products differ from those observed in the section above. Thus, in their SEM images, the following nanoparticles are observed: magnesium nanoparticles (Fig. **7A**) with a size of 2.0-2.5 μm, zinc nanoparticles (Fig. **7B**) with a size of 0.2-0.4 μm, and copper nanoparticles (Fig. **7C**) with size from 0.2 μm to 0.55 μm. In case of the image with Zn nanoparticles (Fig. **7B**), wire- or tube-like formations are seen, which were later confirmed as carbon nanotubes with a thickness of 25-27 nm and length of 360-400 nm. In a TEM image of the sample ferrocene-CuPc (Fig. **7D**), a thin layer of possible graphene in a corrugated form is observed, which is not totally extended on the sample surface but rather presents

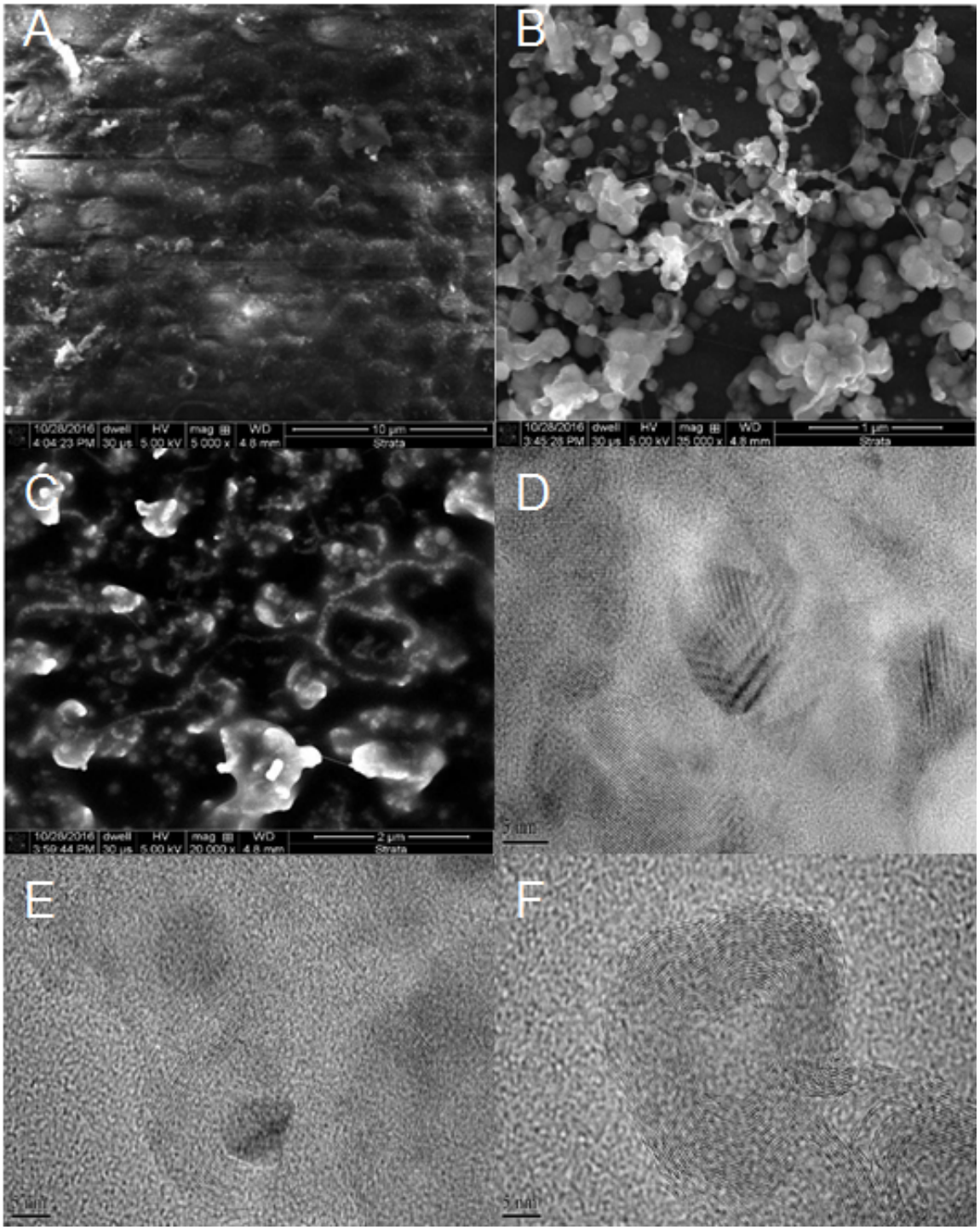

Fig. (7). SEM (**A-C**) and TEM (**D-E**) images of the samples, obtained from: **A**) ferrocene + toluene + MgPc (0.05 wt.%); **B**) ferrocene + toluene + ZnPc (0.05 wt.%); **C**) ferrocene + toluene + CuPc (0.05 wt.%); **D**) ferrocene + toluene + CuPc (0.05 wt.%); **E**) ferrocene + toluene + MgPc (0.05 wt.%); **F**) ferrocene + toluene + NiPc (0.05 wt.%).

small waves in the form of valleys and ridges. The TEM image of the sample prepared from ferrocene plus MgPc (Fig. **7E**) indicates a cross-sectional view of a layer of multi-wall carbon nanotube with internal diameter of 8.33 nm. The TEM image of the sample prepared from ferrocene plus NiPc (Fig. **7F**) shows an MWCNT with an internal diameter of 11.66 nm and external diameter of 33.3 nm and the TEM image of the sample prepared from ferrocene plus ZnPc (Fig. **8**) shows an MWCNT with an external diameter of 12.50 nm. In addition, the formation of aligned carbon nanotubes was observed using the glass of optical fiber and metal phthalocyanines as precursors. Fig. **9** shows the vertical growth of carbon nanotubes. The growth speed of MWCNTs can be controlled by exposition time and is in the range of 175-340 nm/s.

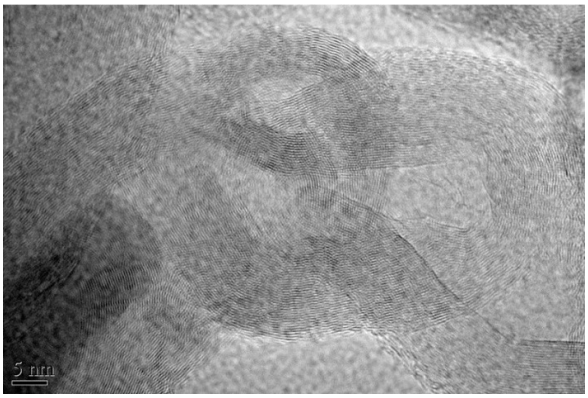

Fig. (8). TEM image of the sample, obtained from ferrocene + toluene + ZnPc (0.05 wt.%).

Fig. **10** shows the Raman spectra for the samples, derived from ferrocene and MPc, indicating that they contain slight differences in comparison with those shown in Fig. (**6**). In relation with band intensities (Fig. **S1**), we note the following. The intensity ratio between the I_D/I_G bands is observed with a higher intensity for the sample, derived from ferrocene + ZnPc (0.74), being compared to ferrocene + NiPc (0.42), ferrocene + MgPc (0.70) and ferrocene + CuPc (0.70) which indicates the presence of dopant material (MPc) present in carbon nanotubes. The intensity ratio changes are directly related to decrease or increase the amount of nitrogen over the CNTs. The presence of bands in an RBM range ($140 \leq a \leq 350$ cm^{-1}) allows us suppose SWCNTs presence, confirmed by the group of very intense bands centered at 200 cm^{-1}, which are characteristic of single-wall carbon nanotubes.

In the Raman spectrum of the CNTs, according to the characteristic bands of these materials and to the intensity ratio between the D and G bands, the degree of graphitization of the walls of the nanotube can be evaluated, as well as the presence of defects in the network of the same. The vibration band G, characteristic of the CNTs, is located at ~1580 cm^{-1} and corresponds to the fundamental vibration (first-order) of tangential elongation and the vibration mode

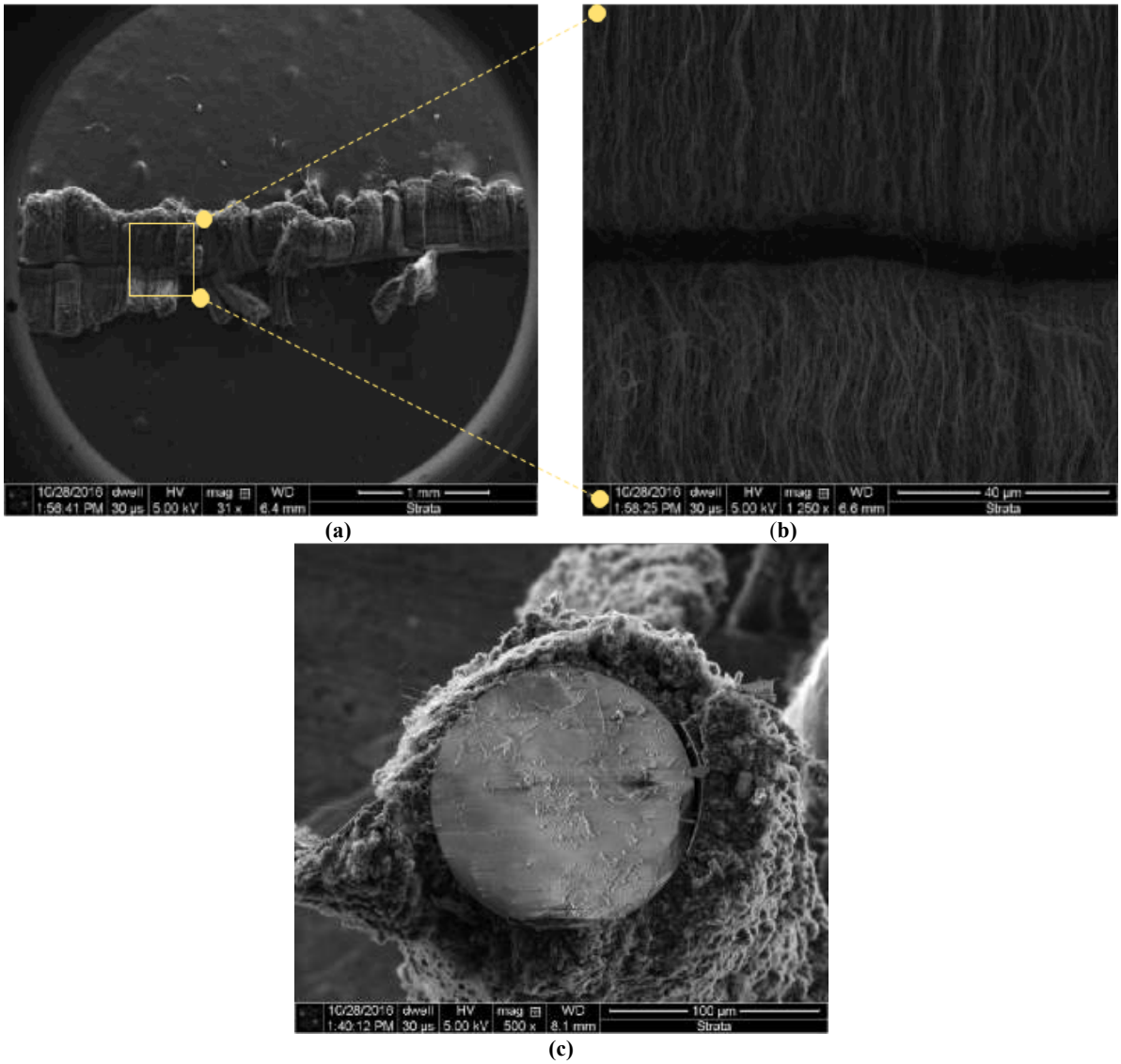

(a) **(b)**

(c)

Fig. (9). a) Transversal cutting of the optical fiber, **b**) inset of the selected section of the Fig. 9a, where a vertical growth of CNTs are seen, **c**) front view of the optical fiber.

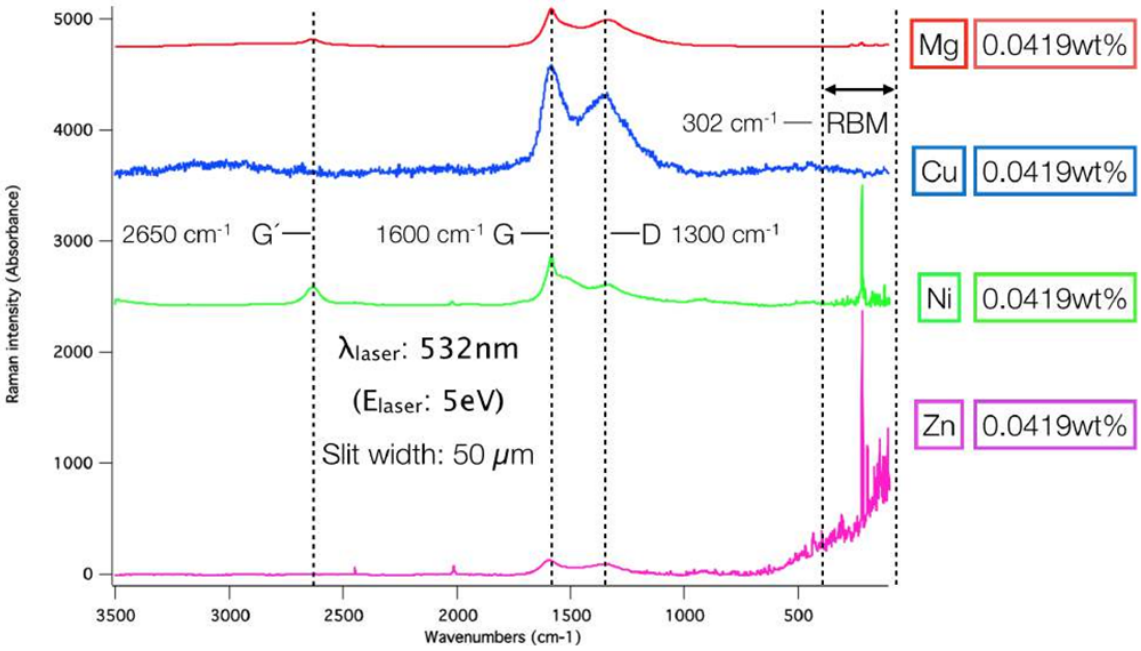

Fig. (10). A comparison of Raman spectra of the samples, obtained from ferrocene and MPc.

E_{2G}. The band D is attributed to the defects and impurities which the nanotube contain in the network; this band is located at ~1330 cm^{-1} and corresponding to the A_{1G} vibration mode, while the G band, located at ~2660 cm^{-1}, corresponds to an over-tone of the mode D. The first band D appears at approximately 1350 cm^{-1}, which indicates the disorder of the graphitic structure. There is a strong increase in the G band at 1600 cm^{-1}; this band is corresponding to the vibration mode A_{1G}. In the ferrocene + NiPc-derived sample and in the ferrocene + MgPc-derived sample (Fig. **S1**), a band appears in 2633 cm^{-1} related to the integrity of the carbon structure, in which confirms the stacking of graphene layers.

3.3. Results of Kelvin (4 Wire Sensing) Measurements of Samples, Obtained from Ferrocene and MPc in Toluene+EtOH

Voltage measurements against the current to a very small scale of the order of nanoamperes in DC were made. The slope of the graph obtained in each of the samples being resistance is in the range of kilo-ohms, is achieved (Fig. **3**). The summary of the readings taken with the technique Kelvin (4 wire sensing) is shown in Table **2**. It was observed that there are three possible scenarios when depositing nanometer-thin layer of material on the substrate borosilicate glass as follows: 1) the nanometer-scale material is deposited on both sides of the substrate, 2) the material is deposited only on one side of the substrate, and 3) the nanometer material is not deposited on any side of the substrate. This depends largely on the location of the substrate within the quartz tube, that is, if nothing is deposited in the terminals, but deposited in the center, it will melt due to the high temperatures handled in the pyrolysis technique. It is recommended to place the substrates at a distance of 15 cm from the outside in the tube. Comparing the measurements of the samples in Table **2**, we found that using only NiPc and MgPc in percentages 0.5 wt.% and 1.0 wt.%, the resistance is relatively very high (from 25 kΩ to 75 kΩ) having a very high current, small but effective from 7.9 nA to 20.6 nA being sufficient to operate MEMs.

3.4. Kelvin (4 Wire Sensing) Measurements of Samples, Obtained from Ferrocene and MPc in Toluene+EtOH

Direct current measurements were made by the Kelvin technique (4 tips) finding a current on a small scale of the order of the microamperes. The slope of the graph obtained voltage *vs.* current in each of the samples was found to be in a range of 15.99 Ω up to 24.77 kΩ and indicates the resistance of the same. The summary of measurements is shown in Table **3**. It can be observed that the greatest resistance is present in the sample that contained the only ferrocene as a precursor (24.77 kΩ) and that it decreases with the presence of MPc (M = Zn, Mg, Ni or Cu), added to the ferrocene in each sample. It was confirmed that copper is one of the best elements for conduction and transmission of the electric current since it presents the least resistance (only 15.99 Ω) compared to the other metals used in this investigation.

Comparing the measurements of the samples in Table 3 against the measurements of the Table 2, we found that using only metal phthalocyanines with toluene, the resistance is relatively very high (from 30 kΩ to 75 kΩ) having a very high current small but effective from 7.9 nA to 20.6 nA being enough to operate a MEMS. On the other hand, using the MPcs + toluene + ferrocene, a remarkable improvement in the resistance is observed since the latter tends to decrease to 24.77 kΩ at 15.99 Ω, with a current greater than 54.38 μA at 513 μA. The graph and table corresponding to each measurement can be seen in Fig. **S2**, where it is appreciated that all the samples have a straight line with a certain slope which indicates the resistance of the nanometric material.

Table 2. Summary of the measurements of four points for the samples, obtained by pyrolysis of MPc dispersion in toluene.

Toluene with	Concentration, wt.%	Initial Voltage µVolts	Final Voltage mVolts	Initial Current nA	Final Current nA	Resistance, kΩ
MgPc	0.5	320	2.79	16.64	100	29.681
	1	226	2.25	20.60	100	25.477
NiPc	0.5	558	61.1	9.40	1000	61.156
	1	393	7.39	7.96	100	75.972
ZnPc	0.5	428	2.47	14.23	100	17.356
CuPc	0.5	341	7.01	21.45	1000	15.34

Table 3. Kelvin (4 wire sensing) measurements of samples, obtained from ferrocene and MPc in toluene.

Toluene with	MPc Concentration, wt.%	Initial Voltage, µv	Final Voltage	Initial Current, µA	Final Current, µA	Resistance
Ferrocene + CuPc	0.05	442	15.56 µv	54.38	1	15.99 Ω
Ferrocene + MgPc	0.05	431	42.16 µv	17.75	1	42.48 Ω
Ferrocene + NiPc	0.05	240	102.12 µv	5.61	1	102.45 Ω
Ferrocene + ZnPc	0.05	397	8.3 v	261.53	1	11.251 kΩ
Ferrocene	0.50	547	10 v	513	917	24.77 kΩ

CONCLUSION

Carbon nanoparticles and nanotubes, both SWCNTs and MWCNTs, can be obtained *via* spray pyrolysis from metal phthalocyanines as precursors of metal particles, playing the role of catalyst for the formation of carbonaceous nanostructures. The presence of ferrocene contributes to the formation of tubular nanostructures. The growth speed of aligned MWCNTs can be controlled by exposition time and is in the range of 175-340 nm/s. SWCNT monolayers have diameters of 1.45 nm. The G, D and G' characteristic bands of SWCNTs were confirmed by Raman spectroscopy, as well as other intense bands in the range of 140 to 350 cm^{-1} corresponding to RBM (radial breathing mode) and a less intensive band intermediate frequency modes (IFM) 750 cm^{-1}, 960 cm^{-1} corresponding to the IFM^{-} and IFM^{+}. Thin layers of nanomaterials, deposited on borosilicate glass, were found to conduct in nanoamper scale, allowing their further use in MEMs devices. Comparing our results with recent other data on other organometallics as catalyst precursors, for example ferrocene and $M(CO)_5(t\text{BuNC})$ (M = Mo, W) as catalyst precursor and toluene as carbon precursor [29], we note that the use of MC does not require temperatures above 760°C, high-cost chemicals and sophisticated equipment. Indeed, this area is not well developed starting from the beginning of this century [30].

CURRENT & FUTURE DEVELOPMENTS

Spray pyrolysis method is currently one of the most common techniques in the synthesis of carbon nanotubes and it needs further development. In particular, a search of new catalyst precursors, rather than commonly used ferrocene, is one of the routes in the investigations in this field. Typical temperatures in these processes are 700-900°C, so the main goal of the catalysis search is the decrease of this value to at least 500°C or lesser (in some industrial applications, the pyrolysis can start even at 250°C), that could be very useful for scaling up this technique. In addition, the production of a more variety of carbon nanotubes depending on reaction parameters (reactor temperature, gas-flow rate and catalyst-carbon precursor ratio) is needed. The formed carbon nanotubes could vary in lengths, wall thickness and internal channel diameters. Successful management of these processes can lead to a cheaper fabrication of distinct types of carbon nanomaterials, from pure hydrocarbons or several low-cost wastes containing them (for instance, used tires, carbon residues in oil refineries, pyrolytic oil and pyro-gas).

ETHICS APPROVAL AND CONSENT TO PARTICIPATE

Not applicable.

HUMAN AND ANIMAL RIGHTS

No Animals/Humans were used for studies that are base of this research.

CONSENT FOR PUBLICATION

Not applicable.

AVAILABILITY OF DATA AND MATERIALS

Not applicable.

FUNDING

None.

CONFLICT OF INTEREST

The authors declare no conflict of interest, financial or otherwise.

ACKNOWLEDGEMENTS

The authors gratefully acknowledge the help of the CONACYT-Mexico for Ph.D. scholarship for Antonio Alanis.

SUPPLEMENTARY MATERIAL

Supplementary material is available on the publisher's website along with the published article.

REFERENCES

[1] Iijima S. Helical Microtubes of Graphitic Carbon. Nature 1991; 354: 56-8.
[http://dx.doi.org/10.1038/354056a0]

[2] Rueckes T, Kim K, Joselevich E, Tseng GY, Cheung CL, Lieber CM. Carbon nanotube-based nonvolatile random access memory for molecular computing. Science 2000; 289(5476): 94-7.
[http://dx.doi.org/10.1126/science.289.5476.94] [PMID: 10884232]

[3] Saito S. Carbon Nanotubes for Next-Generation Electronics Devices. Science 1997; 278: 77-8.
[http://dx.doi.org/10.1126/science.278.5335.77]

[4] Prasek J, Drbohlavova J. Methods for carbon nanotubes synthesis—review. J Mater Chem 2011; 21: 15872-84.
[http://dx.doi.org/10.1039/c1jm12254a]

[5] Liu J, Shao M, Chen X, Yu W, Liu X, Qian Y. Large-scale synthesis of carbon nanotubes by an ethanol thermal reduction process. J Am Chem Soc 2003; 125(27): 8088-9.
[http://dx.doi.org/10.1021/ja035763b] [PMID: 12837063]

[6] Hornbostel B, Haluska M, Cech J, Dettlaff U, Roth S. Arc discharge and laser ablation synthesis of singlewalled carbon nanotubes.Carbon Nanotubes. Springer 2006; pp. 1-18.
[http://dx.doi.org/10.1007/1-4020-4574-3_1]

[7] He JH, Kong HY, Yang RR, *et al.* Review on fiber morphology obtained by the bubble electrospinning and Blown bubble spinning. Therm Sci 2012; 16: 1263-79.
[http://dx.doi.org/10.2298/TSCI1205263H]

[8] Meng Y, Xin G, Nam J, Cho SM, Chae H. Electrospray deposition of carbon nanotube thin films for flexible transparent electrodes. J Nanosci Nanotechnol 2013; 13(9): 6125-9.
[http://dx.doi.org/10.1166/jnn.2013.7651] [PMID: 24205613]

[9] Chen SY, Miao HY, Lue JT, Ouyang MS. Fabrication and field emission property studies of multiwall carbon nanotubes. J Phys D Appl Phys 2004; 37: 273-9.
[http://dx.doi.org/10.1088/0022-3727/37/2/017]

[10] Jasek O, Synek P, Zajıckova L, Elias M, Kudrle V. Synthesis of carbon nanostructures by plasma enhanced chemical vapour deposition at atmospheric pressure. J Electr Eng 2010; 61(5): 311-3.

[11] Aguilar-Elguézabal A, Wilber Antúnez GA, *et al.* Study of carbon nanotubes synthesis by spray pyrolysis and model of growth. Diamond Related Materials 2006; 15(9): 1329-35.
[http://dx.doi.org/10.1016/j.diamond.2005.10.011]

[12] Annu A, Bhattacharya B, Singh PK, Shukla PK, Rhee HW. J Alloys Compd 2017; 691: 970-82.
[http://dx.doi.org/10.1016/j.jallcom.2016.08.246]

[13] Sathiskumar C, Karthikeyan S, Roddatis V, Karthik M. Facile and large scale fabrication of thick walled carbon nanotubes by using waste tire pyrolysis oil as carbon feedstock. Mater Focus 2015; 4: 307-12.
[http://dx.doi.org/10.1166/mat.2015.1248]

[14] Parasuram B, Sundaram S, Sathiskumar CS, Karthikeyan S. Synthesis of multi-walled carbon nanotubes using tire pyrolysis oil as a carbon precursor by spray pyrolysis method. Inorg Nano-Met Chem 2018; 48: 103-6.
[http://dx.doi.org/10.1080/24701556.2017.1357578]

[15] Nilson K, Ahlund J, Shariati M, *et al.* Rubidium Doped Metal-Free Phthalocyanine Monolayer Structures on Au(111). J Phys Chem C 2010; 114: 12166-72.
[http://dx.doi.org/10.1021/jp910180y]

[16] Das S, Magut PKS, Zhao L, *et al.* Multimodal theranostic nanomaterials derived from phthalocyanine-based organic salt. RSC Advances 2015; 5: 30227-33.
[http://dx.doi.org/10.1039/C5RA00872G]

[17] Gottfried JM. Surface chemistry of porphyrins and phthalocyanines. Surf Sci Rep 2015; 70(3): 259-79.
[http://dx.doi.org/10.1016/j.surfrep.2015.04.001]

[18] Mani V, Devasenathipathy R, Chen SM, Gu JA, Huang ST. Synthesis and characterization of graphene-cobalt phthalocyanines and graphene-iron phthalocyanine composites and their enzymatic fuel cell application. Renew Energy 2015; 74: 867-74.
[http://dx.doi.org/10.1016/j.renene.2014.09.003]

[19] Wang Y, Chen HZ, Li HY, Wang M. Fabrication of carbon nanotubes/copper phthalocyanine composites with improved compatibility. Mater Sci Eng B 2005; 117(3): 296-301.
[http://dx.doi.org/10.1016/j.mseb.2004.12.007]

[20] Kharissova OV, Dias HVR, Kharisov BI, Jiang J. Preparation of carbon nano-onions by the low-temperature unfolding of MWCNTs *via* interaction with theraphthal. RSC Advances 2015; 5: 57764-70.
[http://dx.doi.org/10.1039/C5RA07687K]

[21] Method and device for depositing carbon nanotubes or nitrogen-doped carbon nanotubes by means of pyrolysis CN1678523A, 2005.

[22] Someya M, Fujii T, Hirata M, Horiuchi S. Process for producing aligned carbon nanotube films US6967013B2, 2005.

[23] Preparation method of tetrafluoropropoxy-substituted metal phthalocyanine/carbon nanotube composite material CN103787302B, 2014.

[24] In-situ preparation method of zinc phthalocyanine/carbon nanotube composite catalyst based on solvothermal method CN104959166A, 2015.

[25] Metal phthalocyanine/carbon nano tube composite catalyst and its preparation method and lithium/thinly chloride battery using the catalyst CN101507930A, 2009.

[26] Preparation of electrochemical sensor by loading metal phthalocyanine on carbon nanotube fiber CN107247081A, 2017.

[27] Dresselhaus MS, Dresselhaus G, Jorio A, Souza Filho AG, Saito R. Raman spectroscopy on isolated single wall carbon nanotubes. Carbon 2002; 40: 2043-61.
[http://dx.doi.org/10.1016/S0008-6223(02)00066-0]

[28] Temple PA, Hathaway CE. Multiphonon Raman Spectrum of Silicon. Phys Rev B 1973; 7: 3685-97.
[http://dx.doi.org/10.1103/PhysRevB.7.3685]

[29] Sarah Mohlala M, Liu XY, Robinson JM, Coville NJ. Organometallic Precursors for Use as Catalysts in Carbon Nanotube Synthesis. Organometallics 2005; 24(5): 9726.

[30] Teo KBK, Singh C, Chhowalla M, Milne WI. Catalytic synthesis of carbon nanotubes and nanofibers. 2003.